New Beam Delivery System Optics: *BDS9901*

Peter Tenenbaum
LCC-Note-0020
14-July-1999

Abstract

We describe in detail the optics and XSIF decks for the NLC Beam Delivery System in its present version, *BDS9901*.

1 Introduction

In this Note, we describe the present optics design of the NLC Beam Delivery System, which has been somewhat revised for 1999. Most important optical changes include:

- Organization of BPMs into quad-style (BPMQ), BPMs in feedback loops (BPMFB), BPMs which provide sub-train/multibunch information (BPMMB), and BPMs used to measure beam-beam deflections (BPMIP)
- Addition of a number of small quad, skew-quad, sextupole, and skew-sextupole tuning magnets
- Addition of actuators for the feedbacks
- A 6-quadrupole final telescope, which allows all of the linear degrees of freedom to be optimized
- Replacement of the low-energy final quads Q1A and Q1B with a single magnet
- An improved IP Switch which increases the x distance between the beamlines
- Optimized final focus bandwidth.

In addition to optical refinements, there have been a number of organizational improvements to the decks, and the treaty points in the decks have been made identical to the treaty points in the WBS.

2 Boundaries and Treaty Points

The Beam Delivery System contains 2 subregions: the *collimation section* (`col`), and the *Interaction Region Transport section* (`irt`). The collimation section begins at the upstream face of the first quadrupole in the post-linac dogleg, Q703; it ends at the downstream face of the last quad which is common to the IP1 and IP2 lines, QMB2. The interaction region transport line begins at the downstream face of QMB2 and ends at the interaction point.

One of the requirements of the Beam Delivery System is that it permit the construction and use of 2 interaction points, separated in x by approximately 40 meters and in y by approximately 300 meters. This requires a convention regarding which beamlines are the longer ones and which ones bend to the left or right. The convention agreed upon is that [1]:

- the *electron* beamline going to *IP1* and the *positron* beamline going to *IP2* are *long* beamlines

- Long beamlines have an IP Switch/Big Bend which curve to the *left* when viewed from upstream, and in these lines the value of η_x is *negative*.

The Twiss parameters for the full Beam Delivery System are shown in Figure 1. The beamline used is one of the ones with a long IP Switch.

3 Magnet Families

Table 1 shows the parameters of the magnet families used in the Beam Delivery System. There are 6 families of main quadrupole, 3 families of bend magnet, and 3 families of sextupoles. In addition, there is a family of small quads used for optical corrections of various kinds and a family of x/ycors used by feedbacks.

Family Name	Magnet Type	Effective Length (m)	Full Aperture or Full Bore (cm)
QBDS1	Quad	0.5	1.2
QBDS2	Quad	1.0	1.2
QBDS3	Quad	2.0	1.2
QBDS4	Quad	0.5	3.0
QBDS5	Quad	2.5	1.2
QBDSFT	Quad	1.0	3.0
QTUNE	Quad	0.25	3.0
BBDS1	Bend	2.5	1.27
BBDS2	Bend	2.5	3.0
BBDS3	Bend	3.0	1.27
SBDS1	Sext	0.5	1.2
SBDS2	Sext	0.4	1.2
SBDS3	Sext	0.6	3.0
XCORFBCK	Xcor	0.25	1.2
YCORFBCK	Ycor	0.25	1.2

Table 1: Magnet families used in the Beam Delivery System.

The magnet apertures are chosen to achieve an acceptable beam stay-clear for all energies and all parameter sets once space for the vacuum chamber has been allocated. The vacuum chamber has been assumed to be aluminum, with a 1 mm thickness except in the final doublet, in which a 0.5 mm thickness is used to maximize stay-clears. The stay-clear is 5 σ_x by 36 σ_y in the collimation section, and 14 σ_x by 60 σ_y in the area downstream of the collimation section. Figure 2 shows the beam stay-clear at worst-case beam size (350 GeV CM, normalized emittances of 5 by 0.14 mm.mrad, 0.3% RMS energy spread), along with the vacuum chamber profile. Figure 3 shows a close-up of the final doublet. In the case of the final doublet, the stay-clears are defined by the requirements of the 500 GeV CM optics, rather than 350 GeV CM; at 350 GeV CM the vertical stay-clear is slightly too small in the last lens.

4 Collimation Section

The present design of the collimation section is based upon the ZDR scheme. In the near future a new design with more agreeable optics is expected; in the interim, only minor updates have been performed on the collimation lattice proper, though some changes have been made in the region from the end of the collimation lattice to the beginning of the IRT.

Figure 5 shows the magnet x positions, as a function of z, throughout the collimation section, including the two possible trajectories through the IP switch. The total length of the collimation section is 2534.4 m.

4.1 Post-Linac Dogleg

The post-linac dogleg is required to:

- Provide energy and energy spread diagnostics to the linac when the beam is dumped upstream of the collimators
- Provide a bend geometry which cancels that of the collimator lattice, permitting the net geometry from the linac to the IP switch to be a straight line.

Figure 4 shows the Twiss parameters of the post-linac dogleg. The line has a total length of 112.8 meters, and a net bend of 480 μrad, including a bend of 918 μrad and a reverse bend of 438 μrad. At the point of maximum dispersion (3.2 cm), a laser-wire scanner and a multi-bunch BPM are installed for energy diagnostics. The laser-wire scanner is also supported by an additional free-standing Q-type BPM.

4.2 Collimator Lattice

The NLC collimator lattice is, not surprisingly, the heart of the collimation section. The system performs two iterations of collimation in each plane (x and y) and each phase (interaction-point, or IP, and final-doublet, or FD). The system consists of a dispersion match, four collimation modules separated by $3\pi/2$ phase-advance modules, and a dispersion-suppressor. Figure 6 shows the Twiss functions through the module. The upstream portion of the collimator lattice also includes a septum for extracting beams kicked by the single-beam dumper. The full length of the collimator lattice is 2262 meters.

The ZDR collimator lattice collimates the IP and FD phases at different depths; it is therefore necessary to set the phase advance from this region to the IP properly through all the subsequent matching. For this iteration of the design we have allowed the phase advance to vary freely, since it is expected that in the near future a system with equal collimation depths will be developed, at which time the phase advance requirements will be entirely eliminated.

In addition to the usual instrumentation, each collimator is supported by a free-standing Q-BPM, which is used to control the beam position in the collimator gap.

4.3 Match into IP Switch

The betatron functions at the end of the collimator lattice are quite similar to those at the entrance to the IP Switch; therefore, as shown in Figure 7, a simple 4-quad matching lattice suffices, and only 48 meters is required.

4.4 IP Switch

The purpose of the IP Switch is to provide a sufficient geometrical separation between the beamlines to IP 1 and IP 2 for the two beamlines to coexist. The system consists of 10 bend magnets with a single horizontally-focusing quad in the center, followed by 2 quads which begin the match into the IRT line. The total length of the IP Switch is 111 meters. The unusual pattern of Twiss functions, shown in Figure 8, is designed to minimize emittance growth due to synchrotron radiation. At the end of the IP switch the total separation of the beamlines is 17.6 centimeters, while at the end of the last bend magnet the separation is 15.6 centimeters. This means that the center quad in the system needs to be movable by approximately 6.5 cm on its support when switching beamlines, the last 2 quads must be movable by the aforementioned 17.6 cm, and the bend magnets must have a good-field region of nearly 20 cm, or the bend magnets must also be moved when switching IPs.

Because of its unusual optics the IP Switch provides the best resolution of the beam energy and spectrum. Consequently the center quad contains a multibunch BPM, and a laser-wire and Q-BPM are installed immediately upstream of the quad.

5 Interaction Region Transport

The Interaction Region Transport (IRT) includes the second half of the matching from the IP Switch, an "IP Stretch" module which provides the z separation between IP1 and IP2, the 10 mrad arc (for crossing angles), a full coupling diagnostic and correction section, a geometry-adjustment section, the final focus, and an assortment of matching regions between these. The length of the "long" IRTs (EIRT1 and PIRT2) is 2870 m, while the length of the "short" IRTs (EIRT2 and PIRT1) is 2593 m. The net IP separation in z is therefore 277 meters.

5.1 IP Stretch and Big Bend

Figures 9 and 10 show the Twiss functions for the "short" and "long" Big Bend modules (where the "long" module includes the IP Stretch), respectively. The IP Stretch uses 15 cells of a matched FODO lattice to transport the beam to the Big Bend dispersion-match module; the last 4 quads of the IP Stretch are slightly different in strength from the rest to obtain a perfect match. The short Big Bend is 395 meters in length, while the long one is 672 meters in length (including post-Big Bend matching regions).

Figure 11 shows the geometry of the region from the exit of the IP Switch to the first bend magnets on the short side. The separations are small – a total of roughly 20 cm. Thus it may be necessary, during the operation of one IP, to remove a few magnets which go to the other in order to have adequate clearance. Figure 12 shows the two beamlines on a larger scale. Note that the beamlines will probably need to be housed in a vault from 2500 m to 3000 meters, as the tunnel is expected to have an inner diameter of about 12 feet, and at z=3000 m the beamline separation is up to 4 meters, which is about 13 feet. The switchover point from vault to tunnel is at the z location of the short line's coupling correction section, and the middle of the long line's Big Bend.

The present Big Bend lattice is 15 FODO cells, each of which contains 2 quads and 4 bend magnets. The phase advance per cell is 108° in the horizontal and 90° in the vertical. There is an xcor and a ycor in each of the first 4 cells, for use in feedback; each of the 30 main quads contains a BPM for feedback. There are QTUNE-type quads for horizontal dispersion tuning in cells 9, 10, 14, and 15, and skew quads for vertical dispersion tuning in cells 12, 13, 14, and 15.

5.2 Skew Correction Section and Diagnostic Section

The SCS and the DS are designed to permit full measurement and correction of cross-plane coupling which can have a deleterious effect on the very small vertical emittance. The Twiss functions of the section are shown in Figure 13.

Each section is composed primarily of FODO cells with a 45° phase advance per cell in each plane. This is the optimal phase advance for measurement of uncoupled emittances by 4-wire systems. In addition, each section contains a special module which provides a phase advance of 180° in the horizontal and 90° in the vertical; this unequal phase advance is needed to measure and correct the couplings without degeneracy.

The SCS contains 4 skew quads which are arranged so as to be *orthonormal*: each of the 4 creates coupling at a phase which is not accessible to any of the others, and each of the skew quads has an equal effect on the projected emittances. The DS wires are placed at locations in their lattice which match the skew quad locations in the SCS; however the DS has an additional 2 wires for measuring the in-plane emittances, for a total of 6 laser-wire scanners.

The first wire scanner is located downstream of the last skew quad; thus if the skew quads have properly eliminated incoming coupling, the wires will indeed measure zero cross-plane coupling (as opposed to a system with wires and skew quads interleaved, in which some wires are expected to still show coupling when the beam at the downstream end is uncoupled). This allows coupling correction to be done as a nulling measurement.

Since the laser-wire scanners are expected to have a small region in which the laser light is in focus, each laser wire is supported by a free-standing Q-BPM and horizontal and vertical correctors which are positioned at the optimal phase to steer the beam at the wire. Optimally each wire's Q-BPM and correctors will be in a feedback loop, which will perform a type of "one-to-one" correction in real time. The quad nearest each wire contains a multibunch BPM.

The total length of the SCS/DS complex is 344 meters.

5.3 Geometry Adjustment Section

In order to run the NLC at energies above 1 TeV CM, it is necessary to reduce the bend strength of the final focus bends. This changes the FF geometry; however it is useful to be able to recover a geometry which places the IP at the same location. To achieve this goal the NLC contains an achromatic bend upstream of the final focus, called the Geometry Adjustment Section (GAS). Figure 14 shows the Twiss parameters of the GAS. Figure 15 shows the final focus layout at energies at or below 1 TeV CM, and at energies up to 1.5 TeV CM; for the latter energy the GAS bends are reversed in sign and reduced to 33% of their 1 TeV CM bend angles. Note that some magnets in the final focus will have a movement in x of up to 20 centimeters. The total length of the GAS is 118 meters.

The GAS also contains a pair of correctors used in the final focus launch feedback.

5.4 Final Focus

The Final Focus provides an achromatic demagnification of the beam to the size required at the interaction point (IP). The NLC final focus contains a beta matching region for adjustment of $\beta^*_{x,y}$, horizontal and vertical chromatic correction sections with a beta-exchanger between them, a final transformer, and a final doublet which performs the demagnification. The total length of the final focus is 1736 meters. The Twiss parameters of the final focus are shown in Figure 16.

The final focus is sufficiently complex that its components are worthy of independent consideration in detail.

5.4.1 Beta Matching

The purpose of the beta matching region is to match the linear-optics parameters of the incoming beam to obtain the desired IP parameters. The total number of parameters to be adjusted is 6 (two betatron functions, two waist positions, and the phase advances from the collimator lattice to the final doublet). For complete control of these parameters, 6 quads are needed; the beta match has a total of 7. The beta match also contains a pulsed kicker and a septum for pulse-by-pulse extraction onto a low-power dump, and 2 correctors and 4 BPMs for launch feedback.

5.4.2 Chromatic Correction

The chromatic correction region stretches from the dispersion match after the beta match to the dispersion suppressor upstream of the final transformer. It includes a horizontal chromatic correction section (at the β_x peaks), a beta-exchanger, and a vertical chromatic correction section (at the β_y peaks). Each of the aforementioned regions has a phase advance in horizontal and vertical of 180°, as required for cancellation of the sextupole geometric aberrations introduced when chromaticity is corrected.

In addition to the large chromaticity of the final doublet, each chromatic correction section has a certain internal chromaticity, as do the beta exchanger and the final transformer. Because of these, particles which are off-energy do not see an exact $-I$ transform between the main sextupoles. This chromatic breakdown of the modules upstream of the final doublet limits the bandwidth of the final focus. To correct this, tuning sextupoles are placed at the IP images of the CCX, CCY, and dispersion-suppressor (at each location the β functions are small but the dispersion is nonzero). These "Brinkmann sextupoles" [1] reduce the effect of chromatic breakdown. Figure 17 shows the beam size at the IP for a monochromatic beam, as a function of its centroid energy. The optics and beam conditions for Figure 17 are the 1 TeV CM case "A" parameters ($\gamma\epsilon_{x,y} = 4 \times 0.06$ mm.mrad, $\beta^*_{x,y} = 10 \times 0.125$ mm), and is typical of high-luminosity parameters at assorted energies; the spot size reported is not the conventional RMS beam size, but the "luminosity-equivalent sigma," which de-weights the contributions of the charge in the non-gaussian tails [2]. Figure 18 shows the bandwidth as a function of center-of-mass energy.

The horizontal bandwidth in the present optics is limited by a combination of first- and third-order chromaticity: the unusual behavior of the horizontal spot size in Figure 17 is due to the reduction in β^*_x at lower energies combined with the motion of the waist, which is cubically dependent upon the energy. The vertical chromaticities are extremely small – over the range in Figure 17, the waist moves less than 10% of β^*_y. The limiting issue is a chromogeometric aberration. Figure 19 shows the vertical emittance at the IP as a function of centroid energy for a monochromatic beam.

The performance of the final focus is limited by chromogeometric aberrations, which are most deleterious at low energies (for which the geometric emittance is the largest); it is also limited by synchrotron radiation in the bends and the quads, which are most severe at high energies. Figure 21 shows the luminosity lost, relative to the luminosity expected from linear monochromatic beam transport, as a function of energy. This includes all sources in the IRT, not just the final focus.

As mentioned above, the synchrotron losses in the CCX/CCY bends are unacceptable at energies above 1 TeV. Figure 20 shows the luminosity as a function of the bend angles in the chromatic correction region. For strong bends the luminosity is lost due to SR, while for weak bends the sextupoles are sufficiently strong that chromogeometric effects become dominant. At the optimum value of 40-50% of nominal bend angle, almost all the exptected luminosity is recovered.

[1] Named for DESY physicist R. Brinkmann, who first proposed them.

The ZDR described a feedback which used BPM information at the chromatic correction sextupoles and a pair of quadrupole movers to keep certain parameters of the final focus orbit corrected [3]. The present deck includes FB-BPMs in the appropriate locations, and actuators (modelled as VKICKs in the quads for simplicity) in the necessary quads.

5.4.3 Final Transformer and Final Doublet

The optical functions from the end of the dispersion suppressor to the IP are shown in Figure 22. The present final transformer contains 4 main quads. Using these, the horizontally-focusing quads of the final doublet, and the vertically-focusing superconducting quad of the doublet, it is possible to adjust the 6 independent parameters of the final transformer R-matrix independently. This is important because:

- Since the final quad is a permanent magnet, the optics at each CM energy are different from one another – one cannot simply scale the optics to any energy
- At a minimum the optics must be adjusted to give the correct demagnification, and to position the waist, in each plane (4 parameters total)
- Walker *et al* [4] have shown that the bandwidth of a linear collider final focus depends upon achieving the correct phase advance between the final doublet and the sextupoles, in order to tune the $y'^2\delta^2/x'^2\delta^2$ (U_{3466}/U_{1266}) aberration.

The tuning procedure for the final transformer, final doublet, and the various sextupoles is straightforward but time-intensive. The 6 adjustable final transformer quads are tuned to match the desired IP parameters onto the last sextupole, and also to give a desired horizontal and vertical phase advance (these are set by matching a desired R_{22} or R_{44} from the sextupole to the IP, or equivalently the R_{11} or R_{44} from the IP back to the sextupole). With these settings the sextupoles are tuned to simultaneously minimize the IP spot size and the IP emittance in each plane; finally the bandwidth is measured via tracking studies at the optimum sextupole setting thus obtained. This is repeated for various horizontal and vertical phase advances until a global optimum is found. In practice, there is a tradeoff between the width of the energy "bathtub" and the height of the horizontal spot-size "bump" at positive energy offset: as the overall bandwidth gets larger the bump gets higher, until such time as the bump becomes the limiting factor in the effective bandwidth.

The present optics uses a final lens which is a permanent magnet for all energies. For CM energies of 350 GeV to 750 GeV, the magnet is 2 meters long with a full aperture of 14.4 mm; for energies from 750 GeV to 1 TeV CM, the magnet is 2 meters long with a full aperture of 12.8 mm; in all cases the pole-tip field is 12.5 kG. Because this magnet is not strong enough to provide all the necessary vertical focusing, it is preceded by a 1.5 meter superconducting quadrupole. Table 2 shows the parameters of quad Q1SC. Note that it may be feasible to replace Q1SC with either a powered quadrupole or an adjustable PM quad, at room temperature. This option may require replacement of the Q1SC magnet at 750 GeV CM, at the same time as the Q1 permanent magnet is replaced.

The final transformer also contains the following:

- A special BPM just downstream of Q1, for measuring the beam-beam deflections and for use in various feedbacks
- A crab cavity: the cavity is modelled here as a 36-cell S-Band structure (1.26 meters long), requiring 7.5 MW to achieve a deflecting voltage of 6 MV, based on the ZDR scaling laws [5]

CM Energy (GeV)	Gradient (kG/m)	Minimum full aperture (cm)	Desired full aperture (cm)	Pole field at min aperture (kG)	Pole Field at desired aperture (kG)
350	392	1.40	1.42	2.74	2.78
500	-507	1.42	1.42	3.57	3.57
750L	-1822	1.36	1.42	12.4	12.9
750H	-1582	1.30	1.42	10.3	11.2
1000	-2782	1.26	1.42	17.5	19.8

Table 2: parameters of Q1SC quadrupole.

- Two skew quads at the final doublet: a strong one to correct for rotated quads in the final focus, and a weak one for correction of the solenoid's effects (see below)
- Horizontal and vertical deflectors to control the beam position at the IP
- An insertable stopper which prevents the beam from crossing the IP during tuning
- Two sextupoles for sextupole-aberration control, and also two skew sextupoles.

5.4.4 Interaction Region

The main feature of the interaction region is the detector solenoid. Present estimates indicate that the solenoid field may be up to 6 Tesla [6], and the beam passes through the solenoid at a 10 mrad angle relative to the axis of the solenoid. This can result in luminosity reduction due to the following effects:

- Vertical deflection of the beams at the IP, which prevents collisions
- Vertical dispersion at the IP due to the vertical deflection, which enlarges the beam size
- Emittance growth due to synchrotron emission in a vertical-dispersive region
- Cross-plane coupling from the solenoidal field.

Previous estimates of the solenoid's effects were made for the ZDR using a 4 Tesla field and a hard-edged model (in which the field was 4 Tesla and had no radial component, and fell instantaneously to zero at *z=2* meters [7]. In order to improve the estimate, we utilized a preliminary field map which provides a 6 Tesla field at the IP. Figures 23 and 24 show the z and r components of the field, respectively, as a function of z, along the beam's path. This reduced the severity of the effects: Raubenheimer [8] has shown that the optical effects of an IR solenoid are cancelled at the IP (the fringe fields and the main field cancel), if the solenoid does not contain a quad. Since the field is weak in the vicinity of the Q1 quad (2 to 4 meters from the IP), the solenoid's effects are largely cancelled.

In the present configuration, the effects of the solenoid were cancelled at 1 Tev CM by:

- Energizing the final doublet skew quad to an integrated gradient of 0.12 kG
- Energizing the SCS skew quads to small values to eliminate the remaining coupling (the emittance at the DS is thus increased by approximately 2%)
- raising Q1 by 2.6 microns to restore collisions

- moving the main CCY sextupoles by 1.4 microns each to eliminate the remaining dispersion.

The resulting solution restored 98.5% of the luminosity which was available with the solenoid off. The difference appears to be due to increased synchrotron radiation emittance growth, which is much less severe at lower energies.

One remaining problem is the outgoing trajectory. While the beams collide head-on at the desired location, the beam trajectories have a vertical angle with respect to the detector axis. The solenoid on the outgoing side amplifies the problem; by the time the beam reaches the first extraction quad (6 meters downstream of the IP), the 1 TeV CM beam is 400 microns below the nominal beam elevation and has a down-angle of 68 microradians (note that one of the beams is *below* the nominal and the other is *above* it); both the position and the angle offset are approximately tripled at 350 GeV CM. It will be necessary to configure the extraction line to capture this beam and transport it to the dump, probably by changing the elevation of the first few quads at different energies. Also the detector design must take the electron beam trajectory in the detector into account, as the SR photons will produce a vertical fan inside the detector.

6 Deck Organization and Location

The NLC Beam Delivery System production decks are located at:

/afs/slac/g/nlc/lattice/cd1_09-98/beam_delivery

and are also available from the NLC WWW site.

Historically the BDS decks have been quite complex in their organization. This is partially due to the large number of options in the deck:

- Selection of beamline (electrons to IP 1 or 2, positrons to IP 1 or 2), and the accompanying selection of left- or right-bending Big Bend and long or short IP Switch
- Selection of a CM energy, from 350 GeV to 1 TeV CM
- selection of a doublet configuration (below or above 750 GeV CM)
- selection of an optics configuration (cases A, B, or C from the parameter tables).

The selection of options was accomplished by "commenting-out" all options other than those wanted. This proved to be a tedious and error-prone procedure, as there was no guarantee that an inattentive user would select a consistent set of options (for example one might select the 1 TeV CM optics and the low-energy doublet).

This has been eliminated, and options are now controlled by use of a set of "auxiliary files." These are files which contain the parameters needed to select various options. The full set of NLC BDS optics now consists of:

- The master decks which describe the BDS regions, `irt_500GeV.xsif` and `col_500GeV.xsif`
- A set of auxiliary files which select either a long IP Switch bending to the left or a short one bending to the right
- A set of auxiliary files which select the CM energy

- A set of auxiliary files which set the doublet configuration
- A set of auxiliary files which set the beta match optics (for control of IP beam sizes)
- An auxiliary file with universal definitions for the system.

The main decks are stored in the `prod` subdirectory of the BDS directory, and the auxiliary files are in `xsifaux`. The selection of options is automated in the following way: for every valid combination of options there is a corresponding DIMAD command file in the `dimadcmd` subdirectory; each of these files loads the correct auxiliary files, followed by the main decks, and executes the desired DIMAD commands (the main DIMAD action commands are found in a set of command files in the `prod` directory).

In order to maintain the large set of command files, there are three shell scripts: `makecmdfiles, colcommand, irtcommand.` The user edits the first file (`makecmdfiles`) to set the paths for auxiliary files, main files, output files, etc. When executed (in the C shell), `makecmdfiles` calls `colcommand` and `irtcommand` to automatically generate all of the command files.

7 Acknowledgements

This Note would not have been possible without the assistance, ideas, and hard work of: Reinhard Brinkmann, Paul Emma, Dick Helm, John Hodgson, John Irwin, Yuri Nosochkov, Tor Raubenheimer, Andy Ringwall, Nick Walker, Mark Woodley, and Frank Zimmermann.

References

[1] M. Woodley, private communication.

[2] P. Raimondi and T. Usher, private communication.

[3] NLC ZDR, p. 732.

[4] N.J. Walker *et al*, "Third-Order Corrections to the SLC Final Focus," SLAC-Pub-6206.

[5] NLC ZDR, p. 768.

[6] M. Breidenbach, private communication.

[7] NLC ZDR, p. 773.

[8] T. Raubenheimer, private communication.

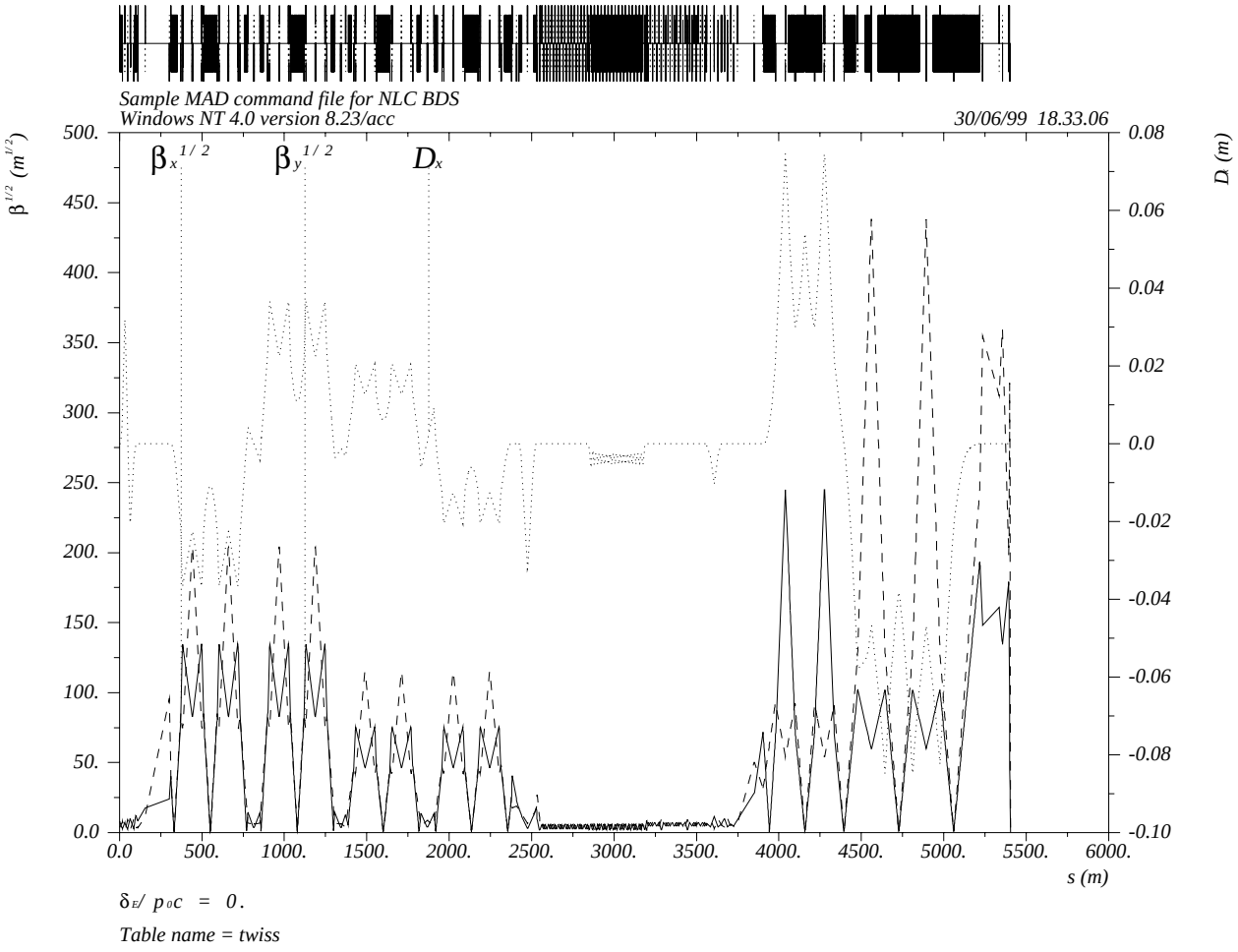

Figure 1: Twiss functions of the full Beam Delivery System.

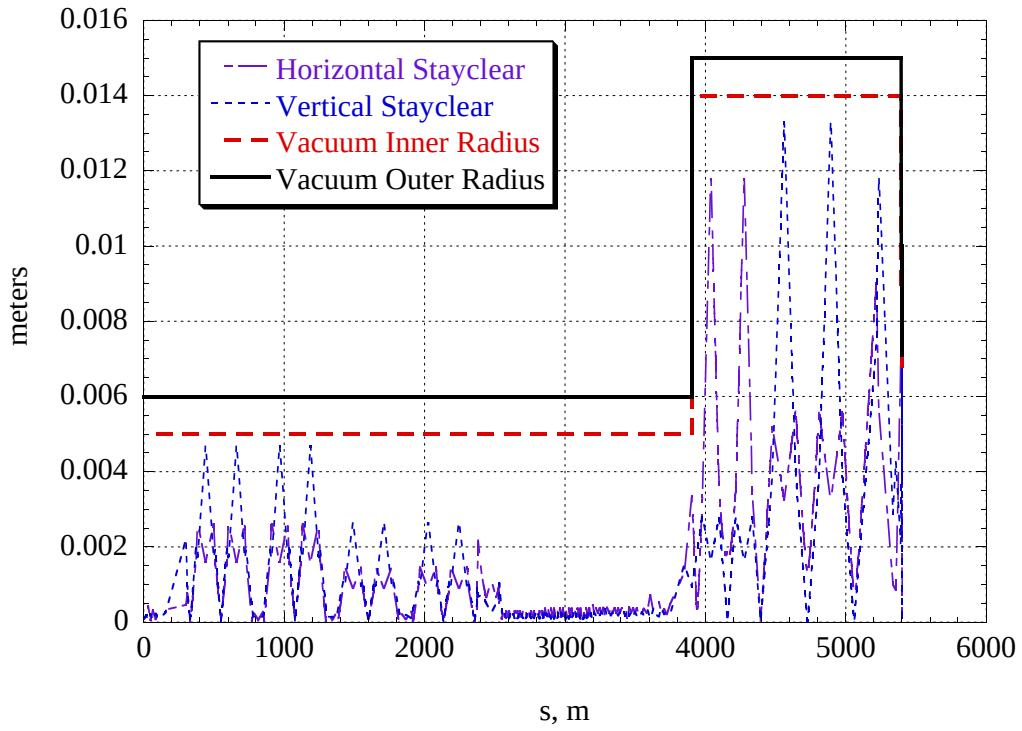

Figure 2: Beam stayclears and vacuum chamber aperture in the beam delivery system for largest emittances at 350 GeV CM.

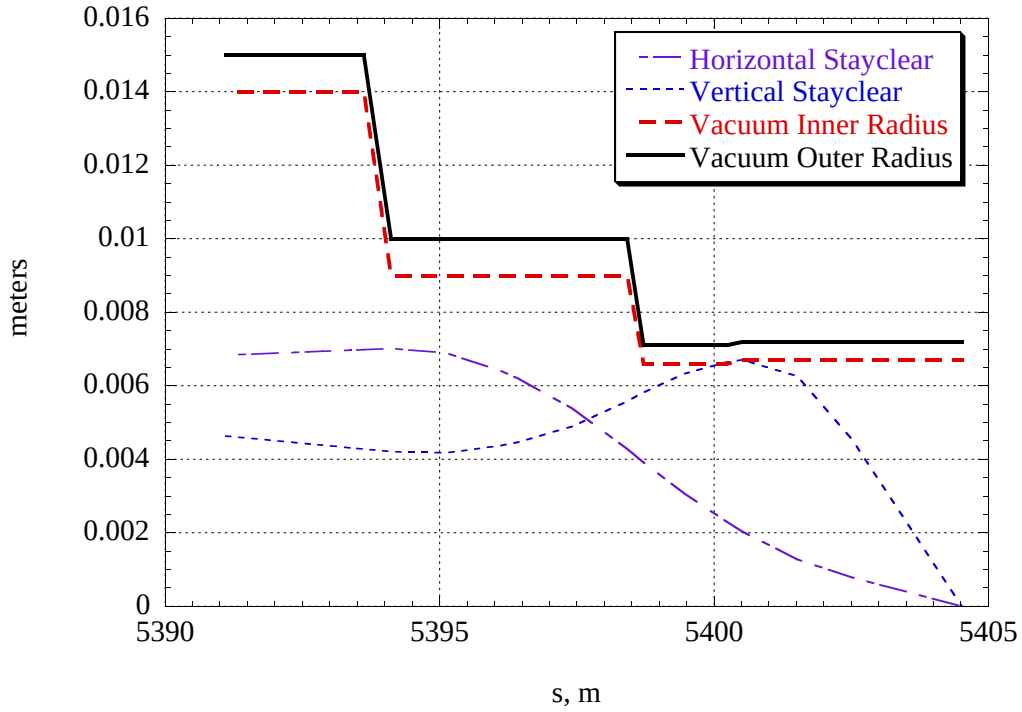

Figure 3: Close-up view of final doublet stayclears and vacuum chamber aperture for largest emittances at 500 GeV CM.

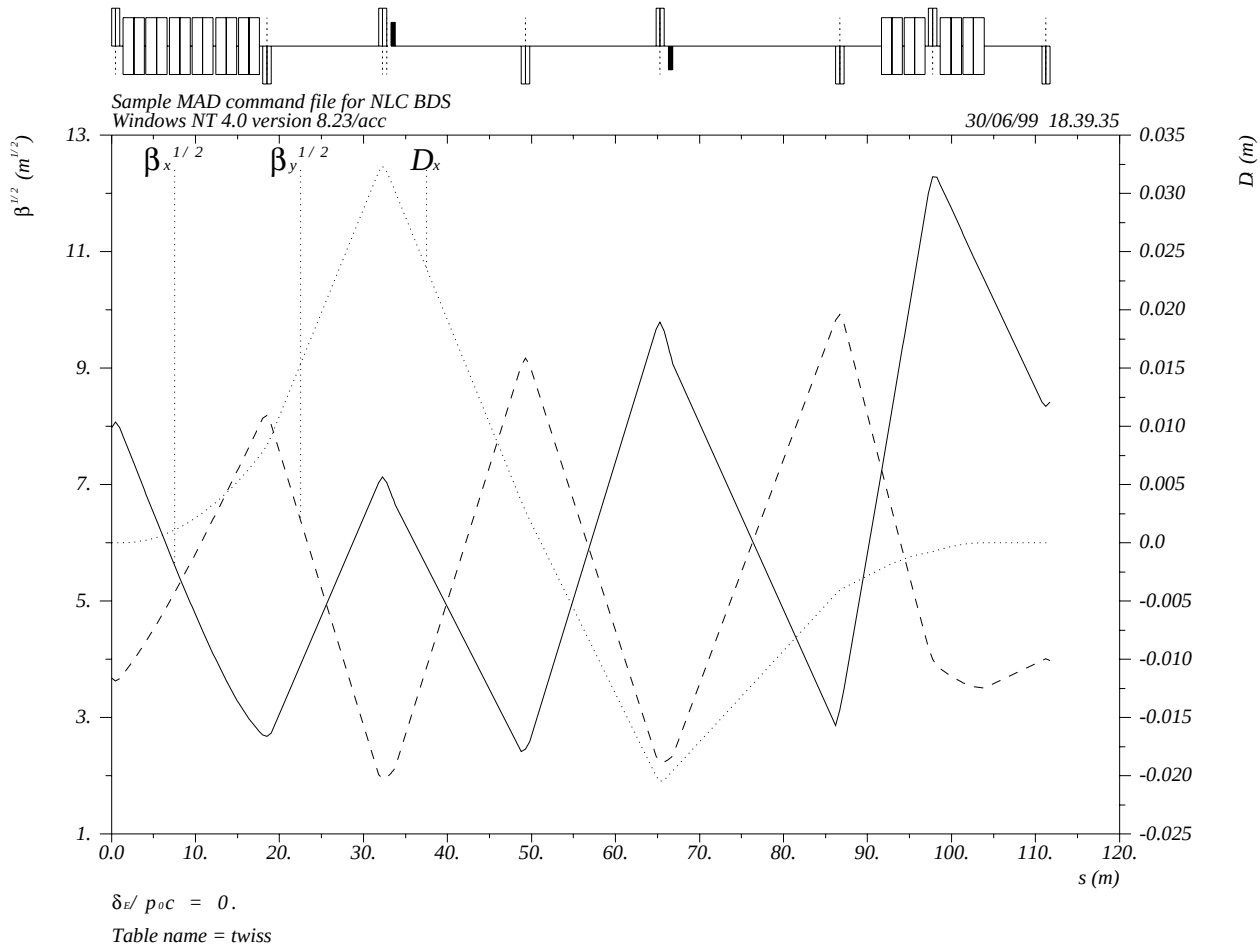

Figure 4: Twiss functions of the post-linac dogleg.

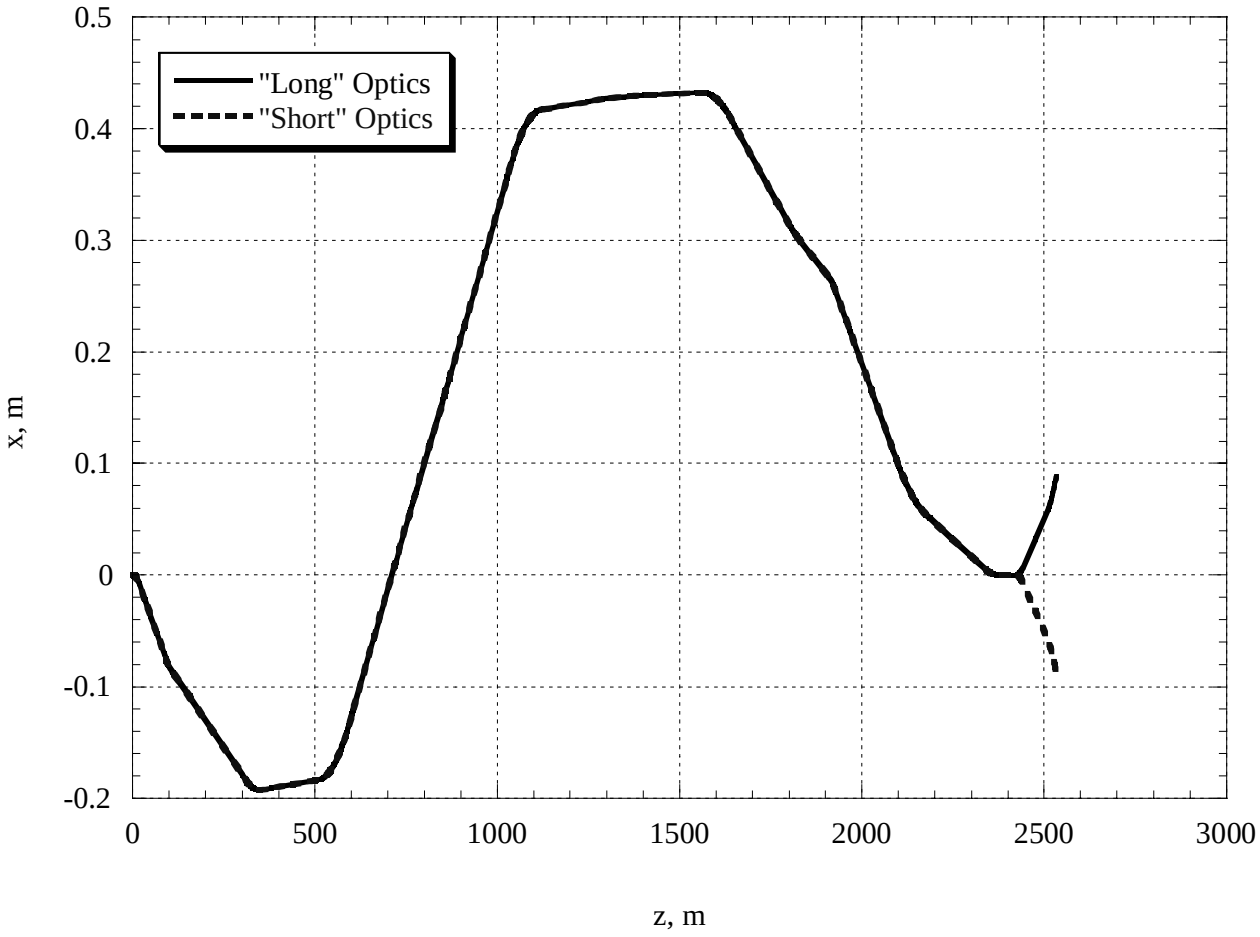

Figure 5: Horizontal positions of collimation system magnets relative to the line of the main linac. Both the "long" geometry (solid) and the "short" geometry (dashed) are shown.

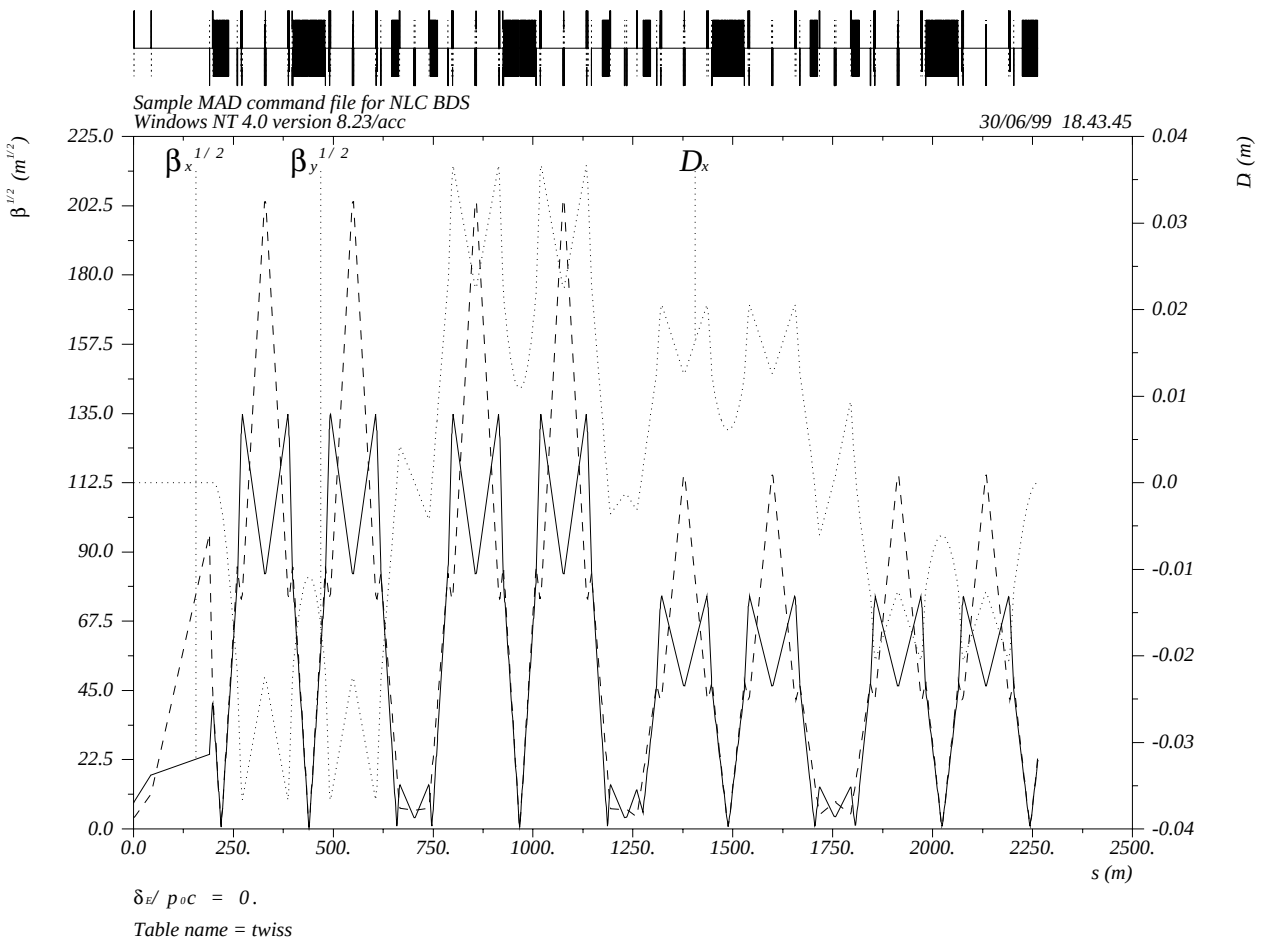

Figure 6: Twiss functions of the collimator lattice

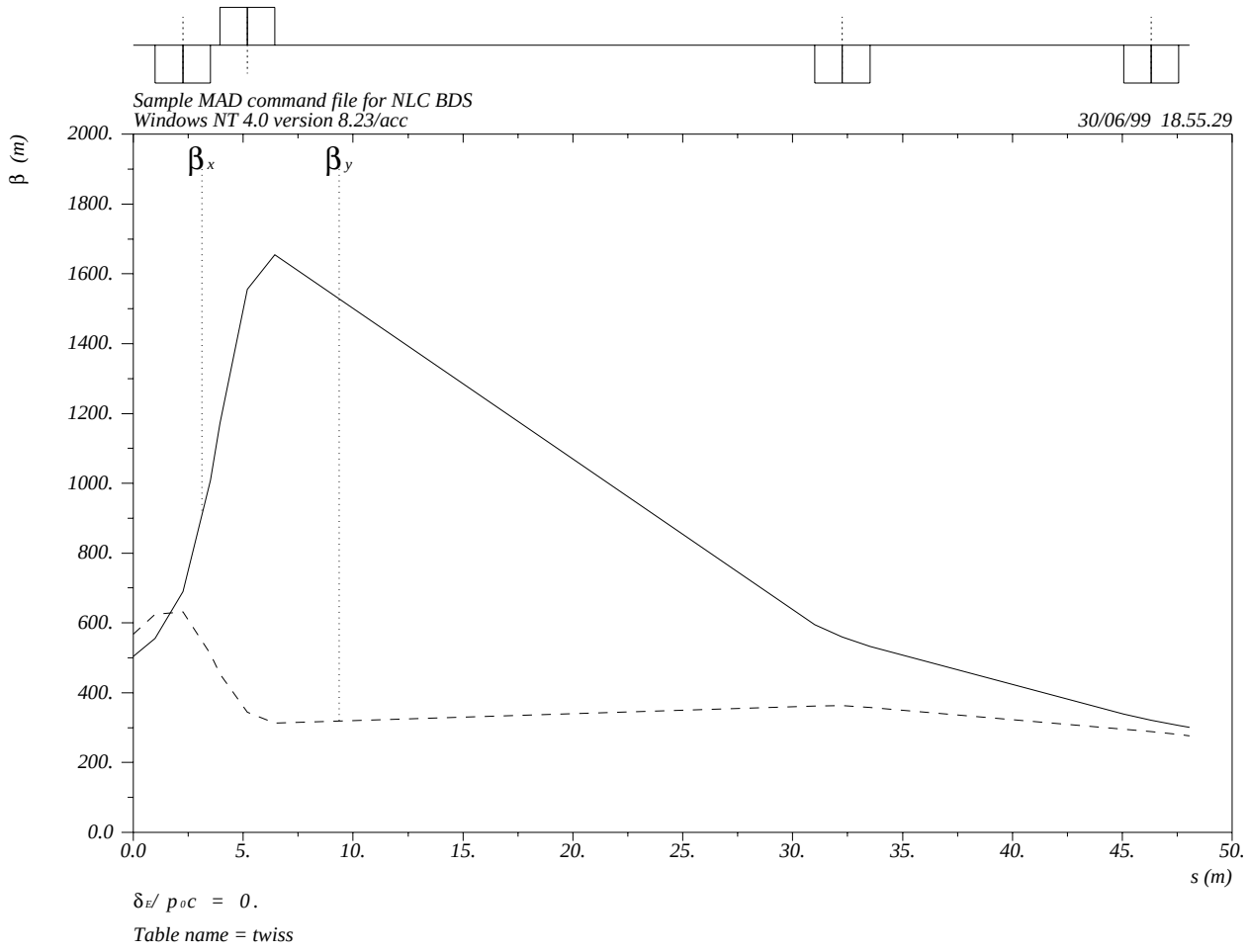

Figure 7: Twiss functions of the collimator-IP Switch matching region.

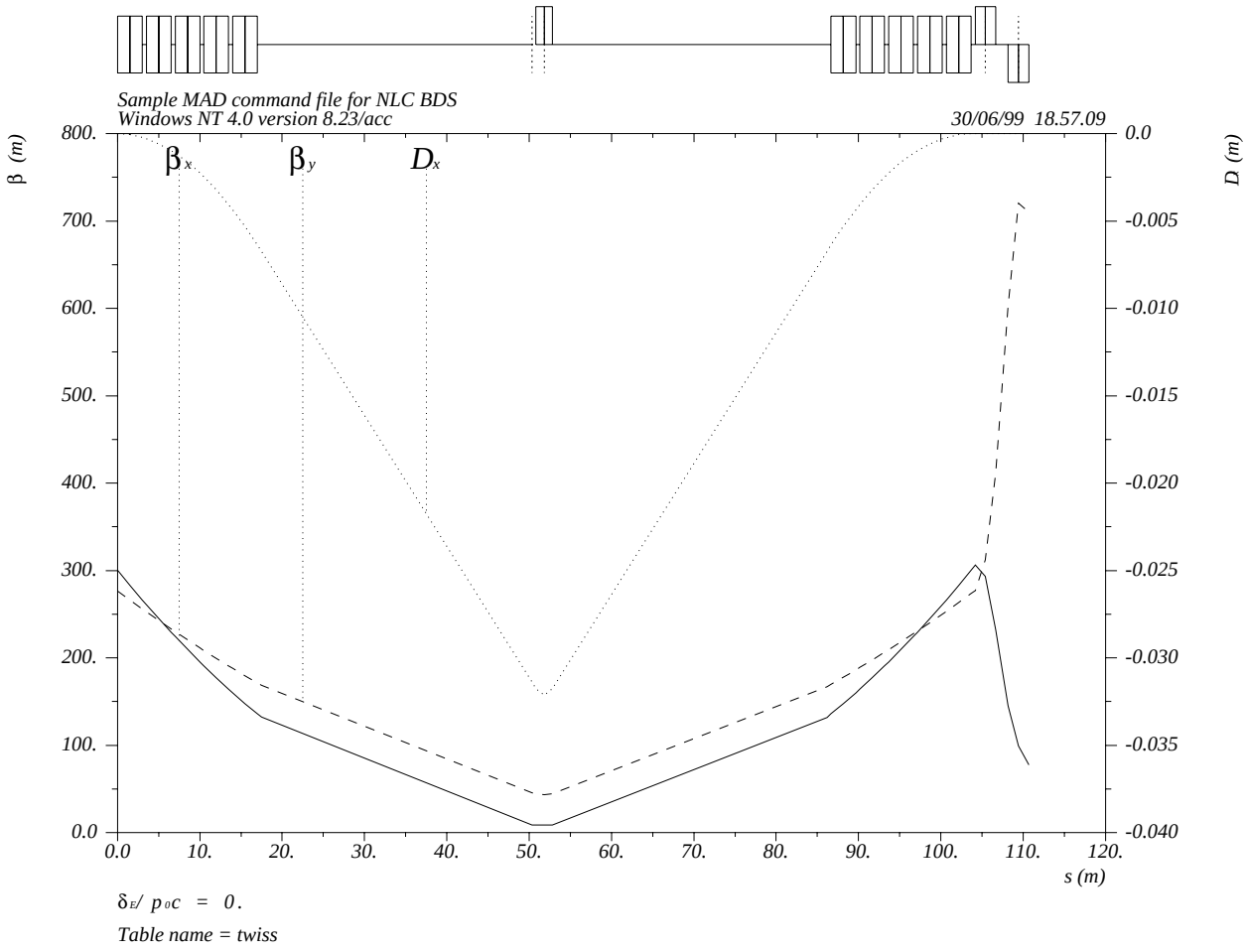

Figure 8: Twiss functions of the IP Switch.

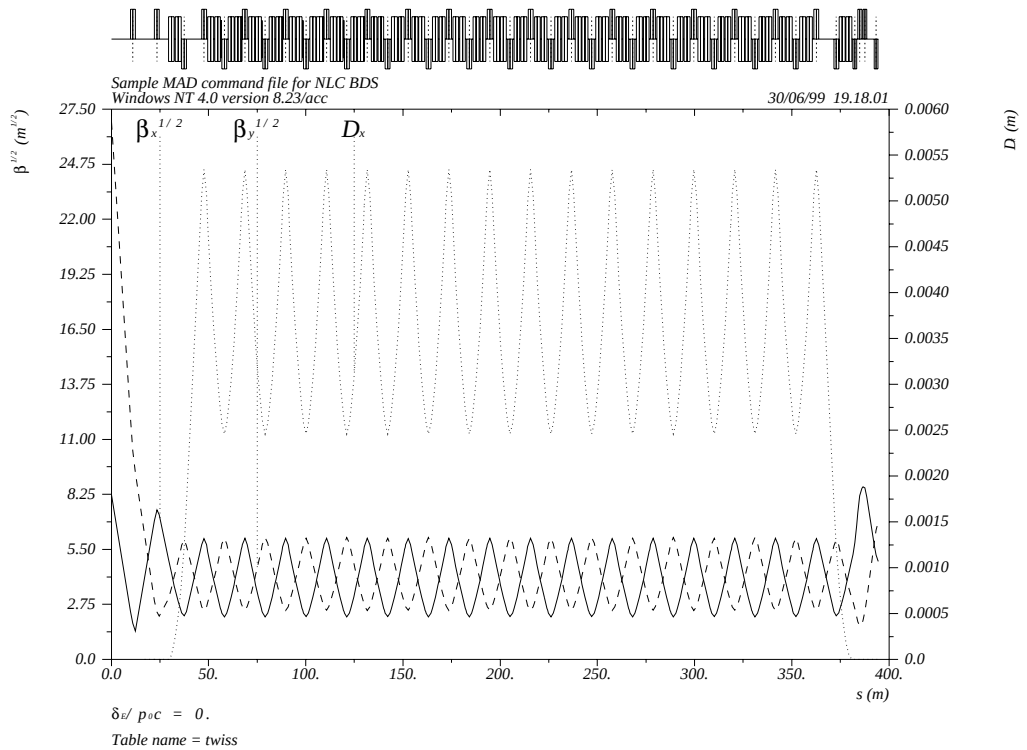

Figure 9: Twiss functions of the "short" Big Bend.

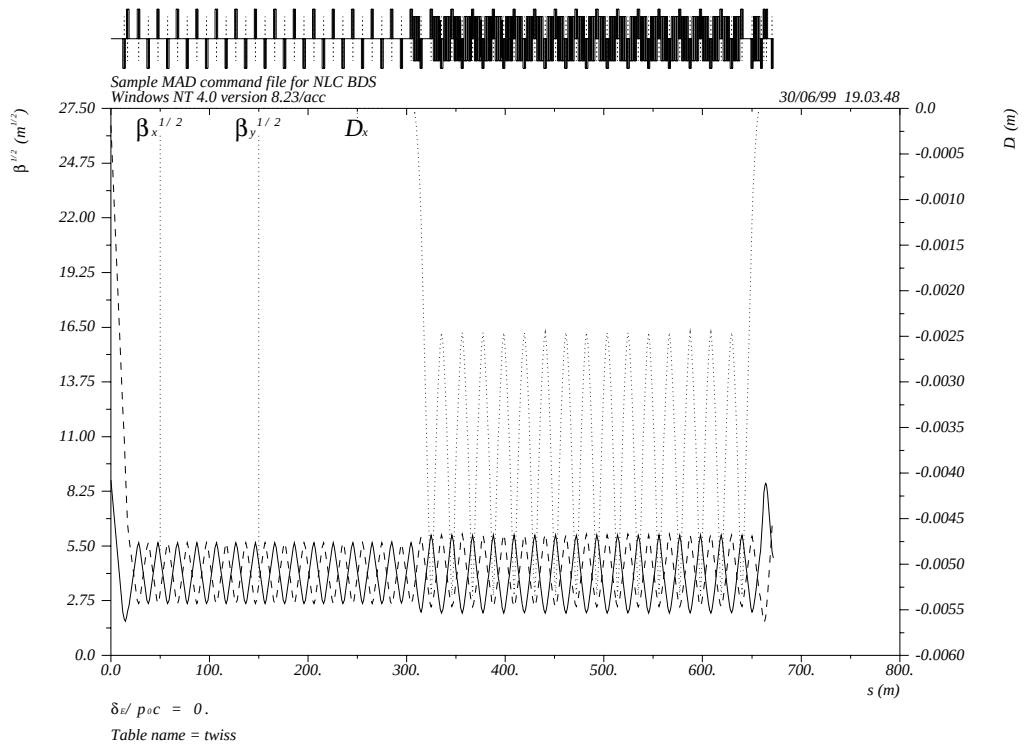

Figure 10: Twiss functions of the "long" Big Bend, with IP Stretch module.

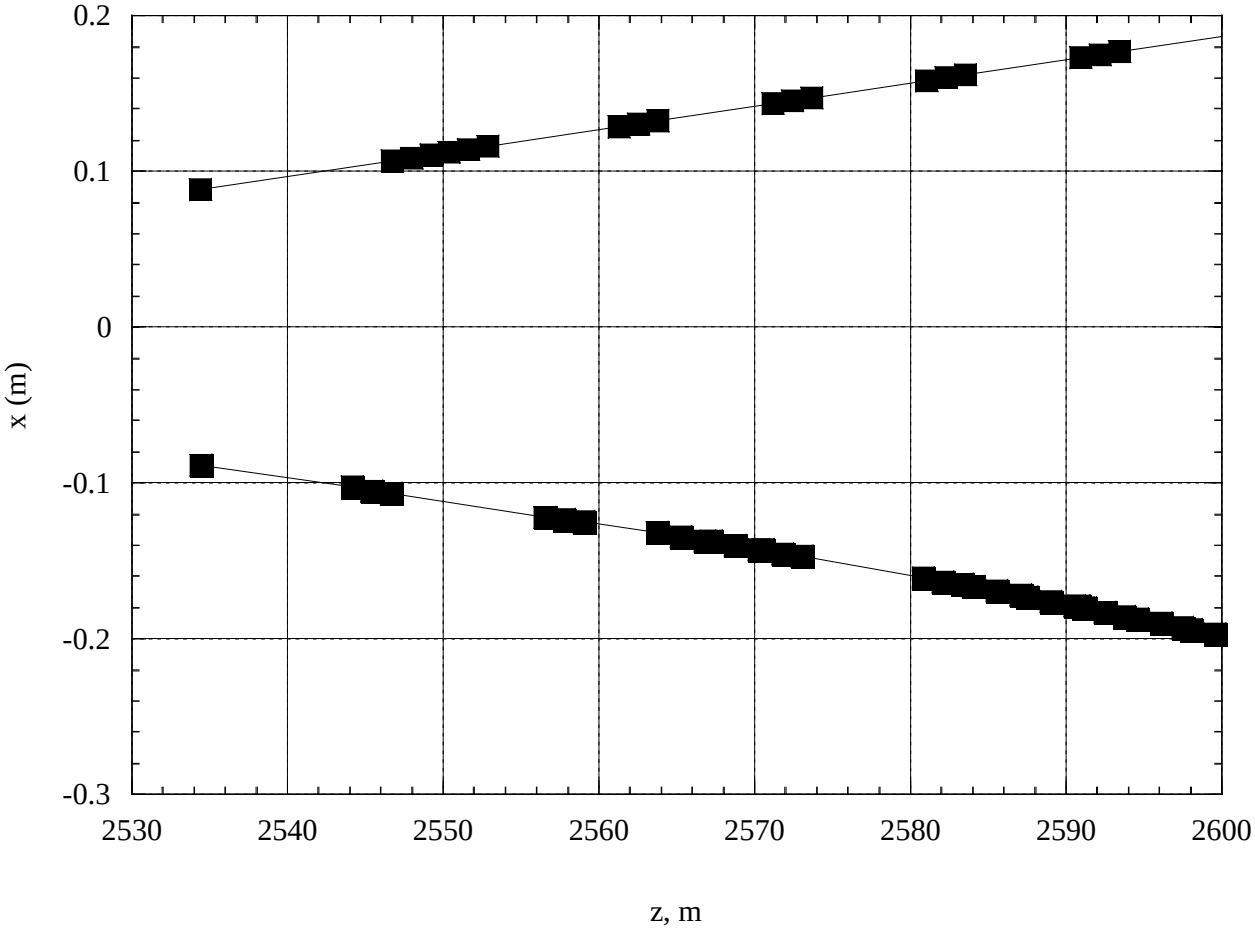

Figure 11: Separated beamlines downstream of the IP Switch. Black boxes denote magnet positions.

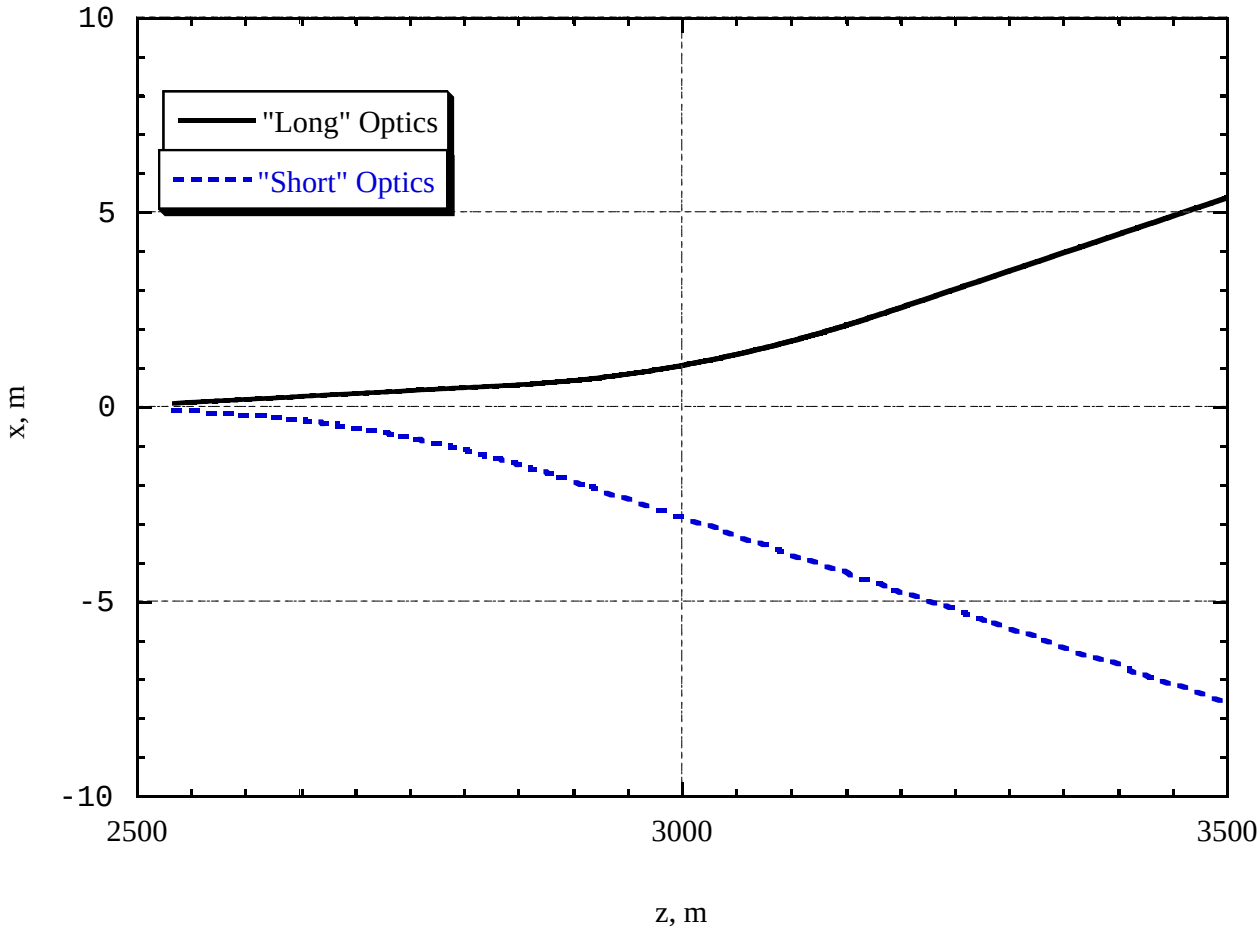

Figure 12: Large-area view of the separated beamlines downstrem of the IP Switch.

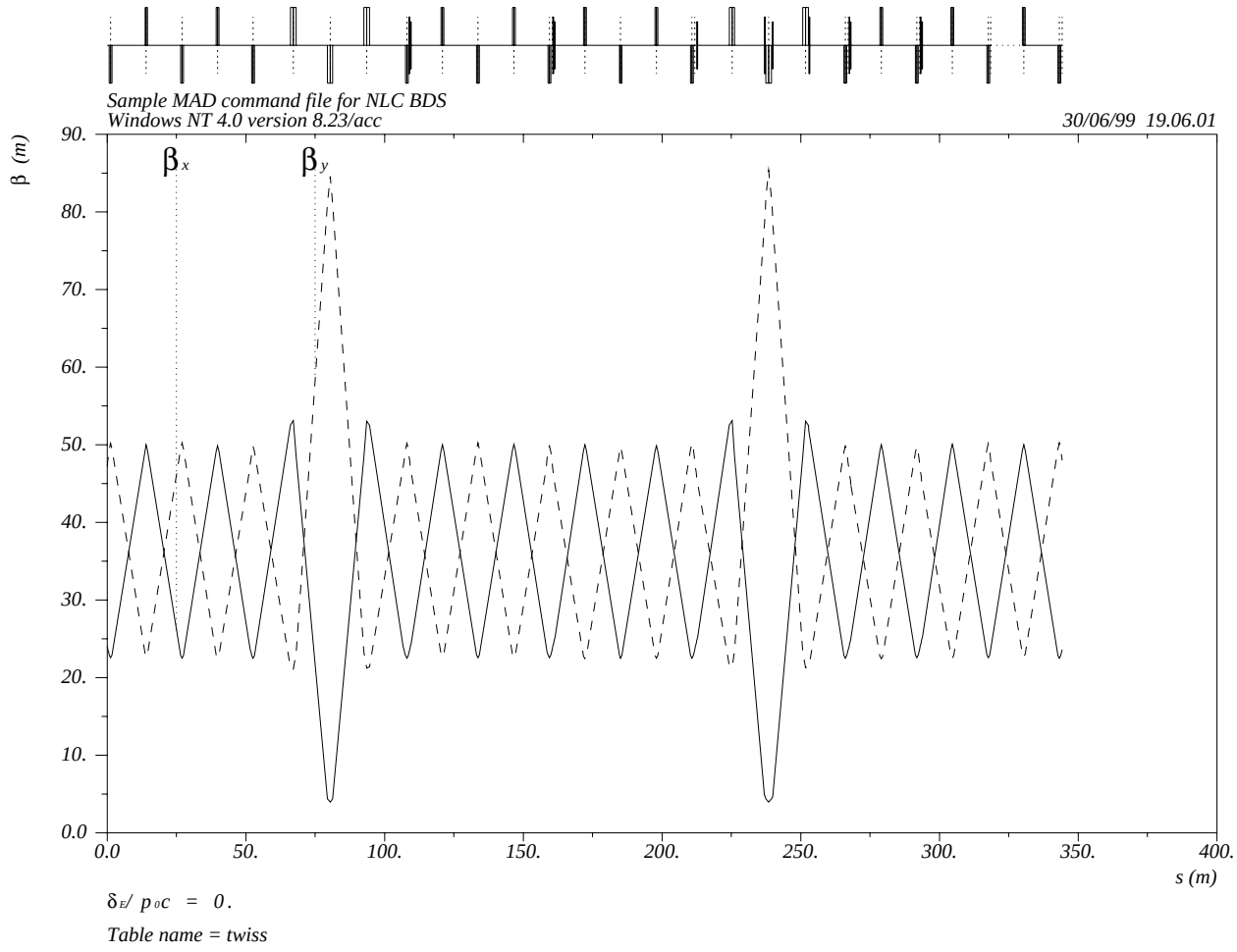

Figure 13: Twiss functions of the Skew Correction and Diagnostic Sections.

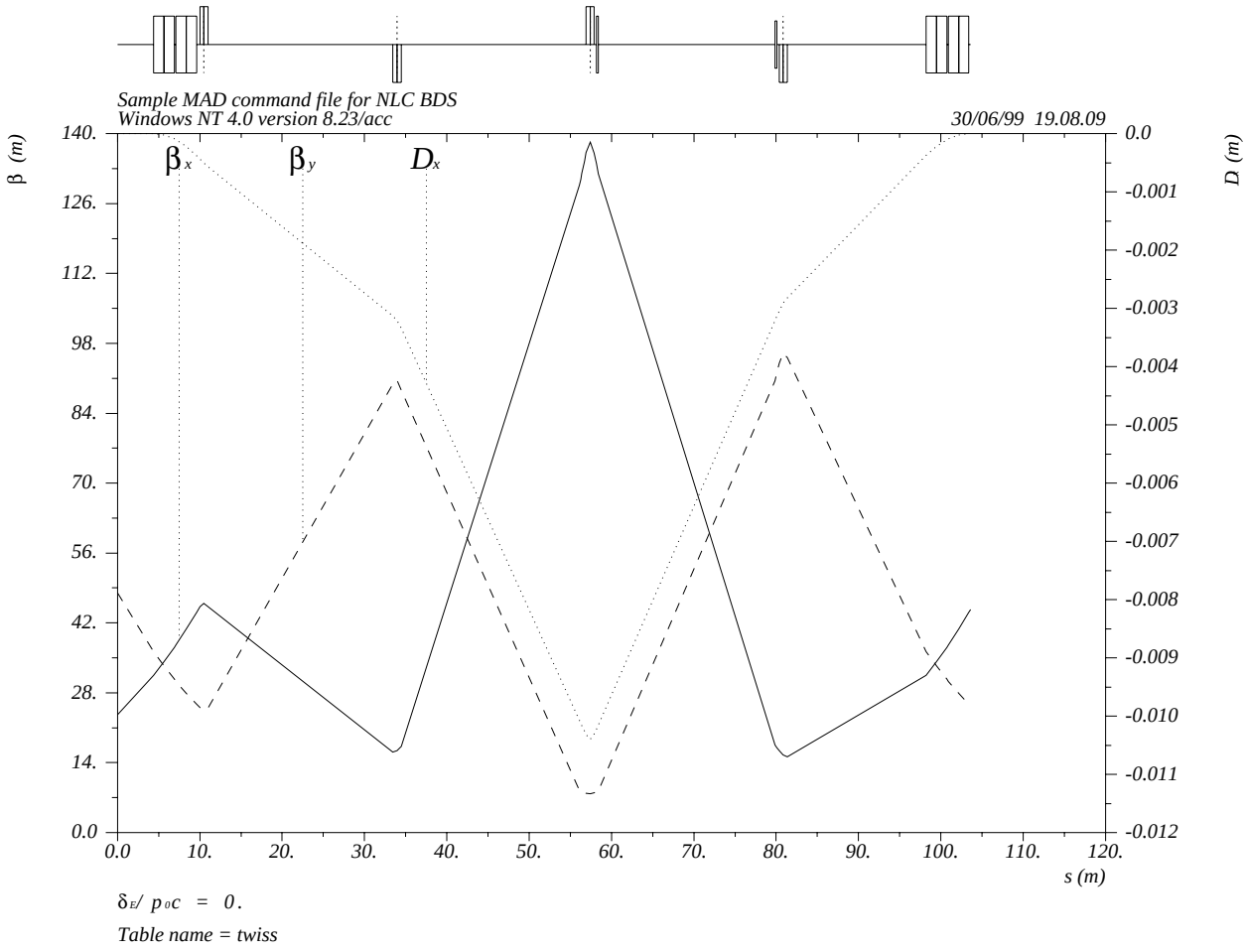

Figure 14: Twiss functions of the Geometry Adjustment Section.

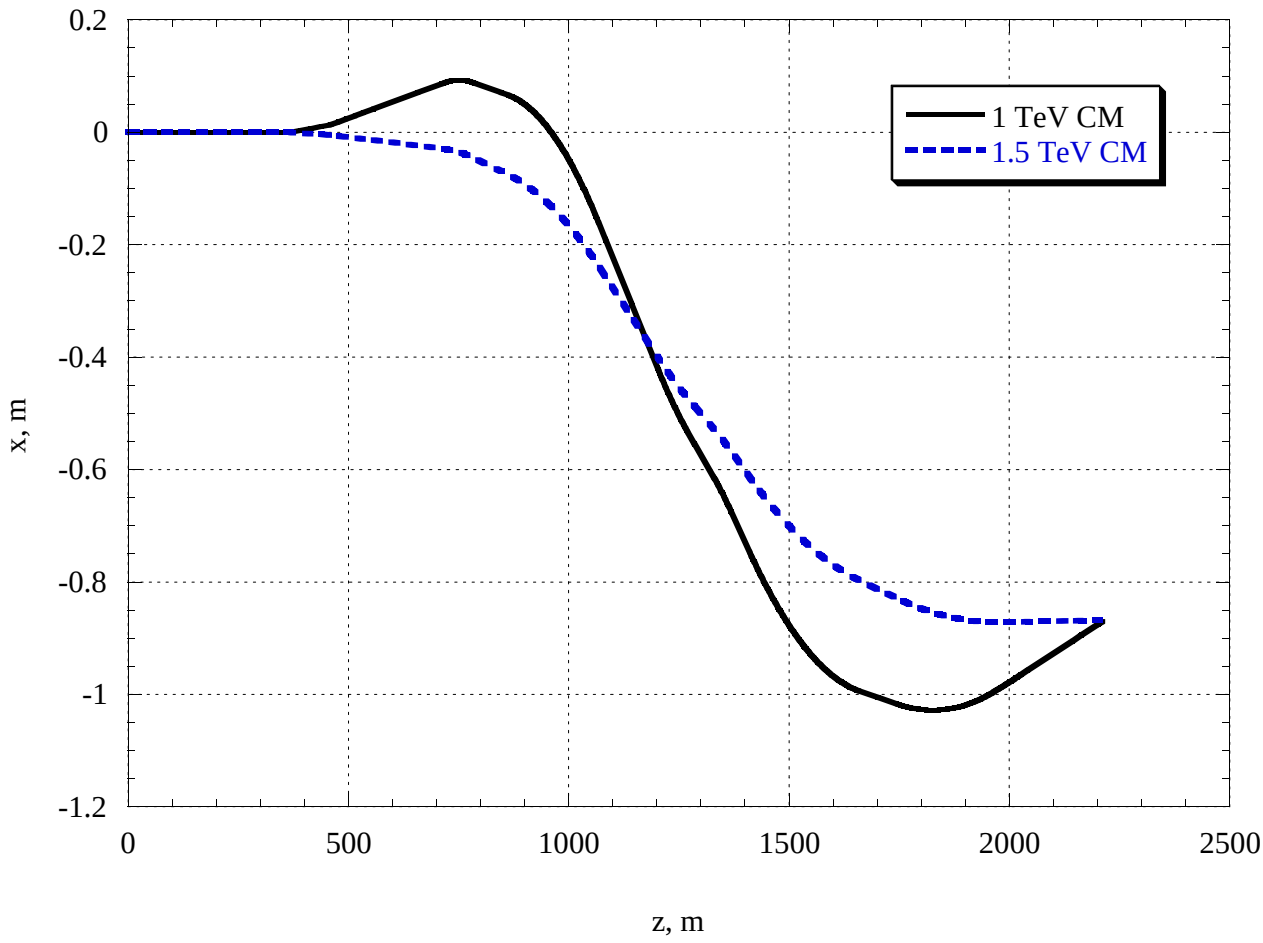

Figure 15: Geometry of the Final Focus for energies below 1 TeV (solid) and above 1 TeV (dashed).

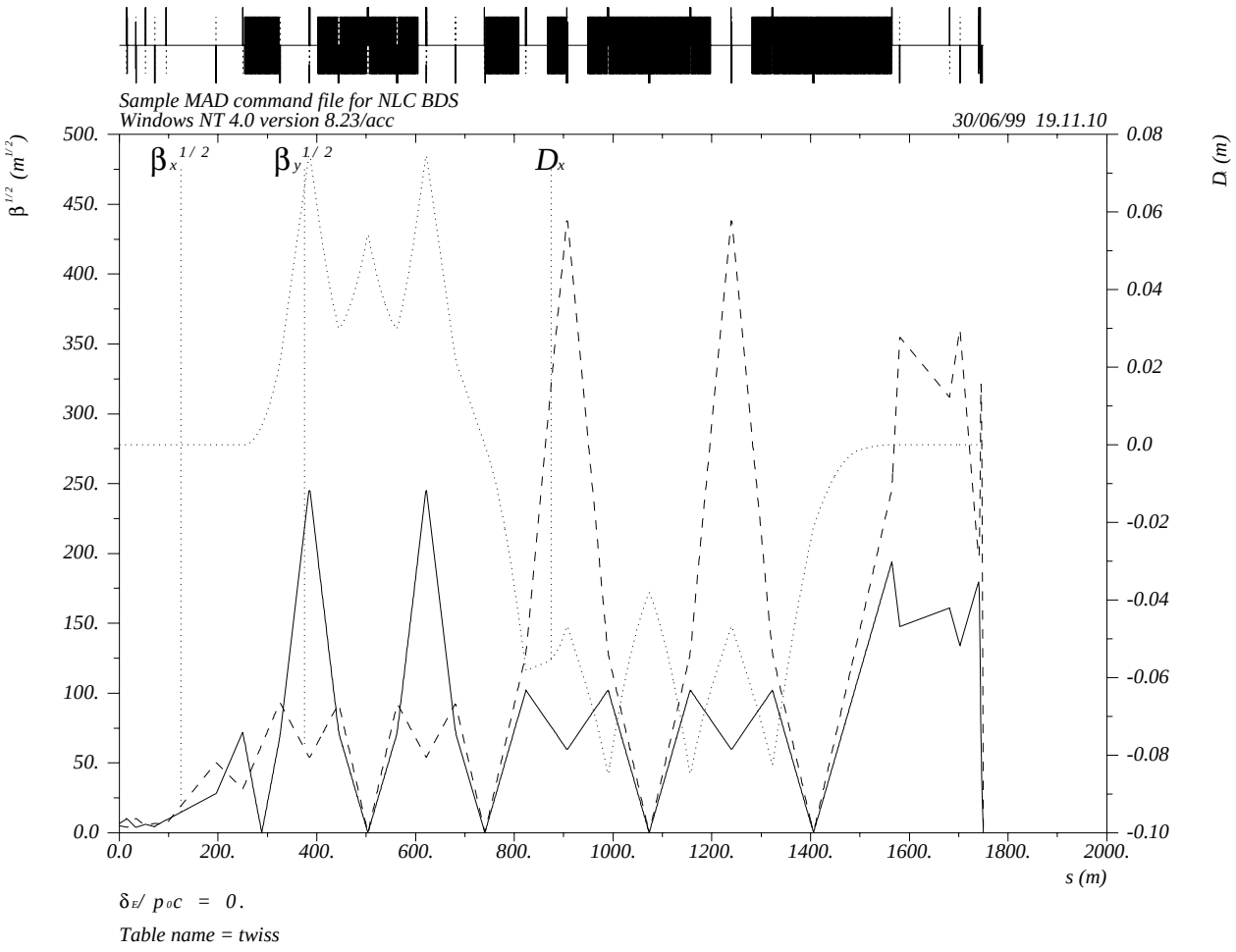

Figure 16: Twiss functions of the Final Focus.

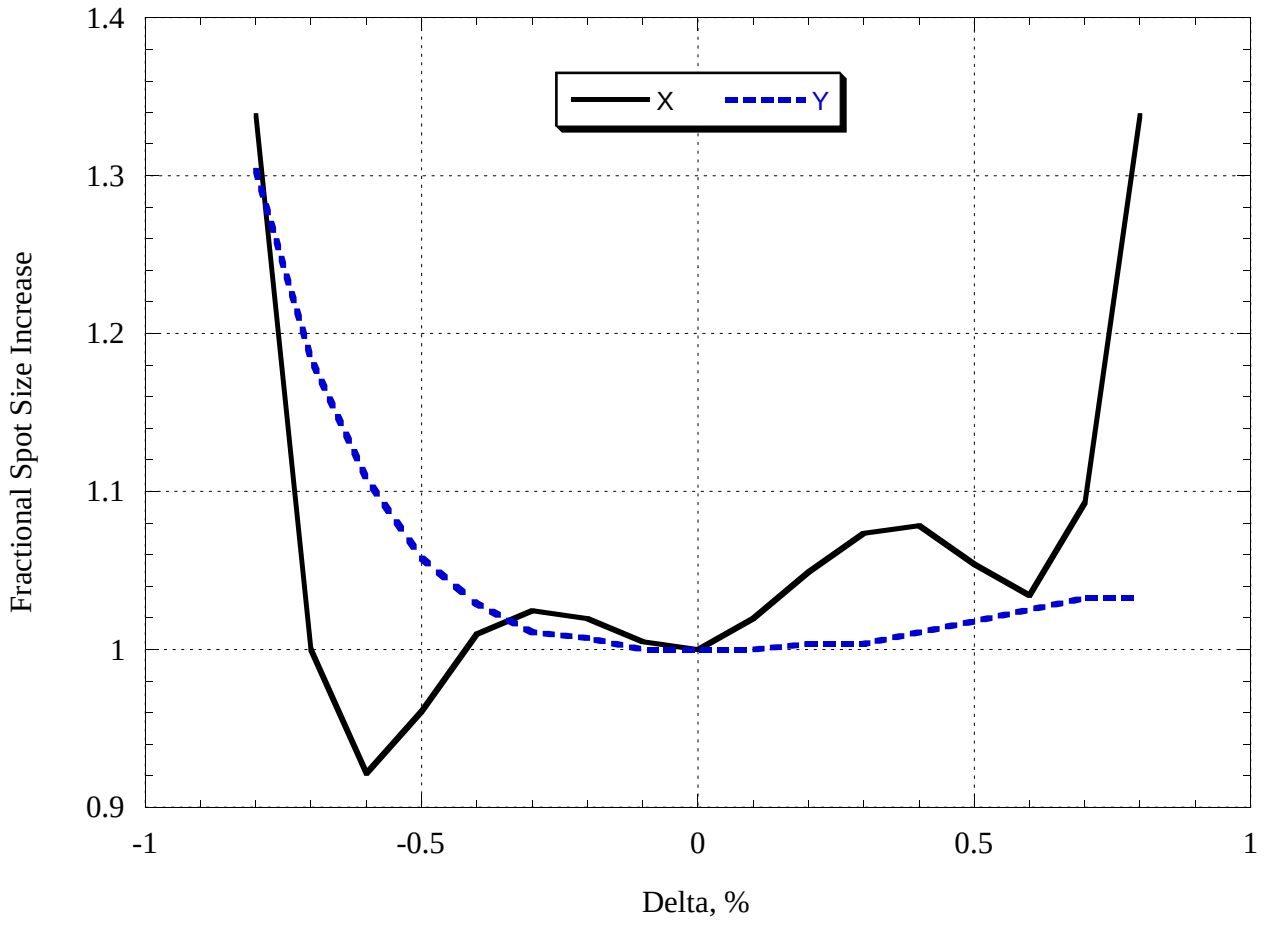

Figure 17: Size of a monochromatic beam at the IP as a function of energy centroid offset. The point at which the nominal beam size is exceeded by 10% is the criterion for the bandwidth.

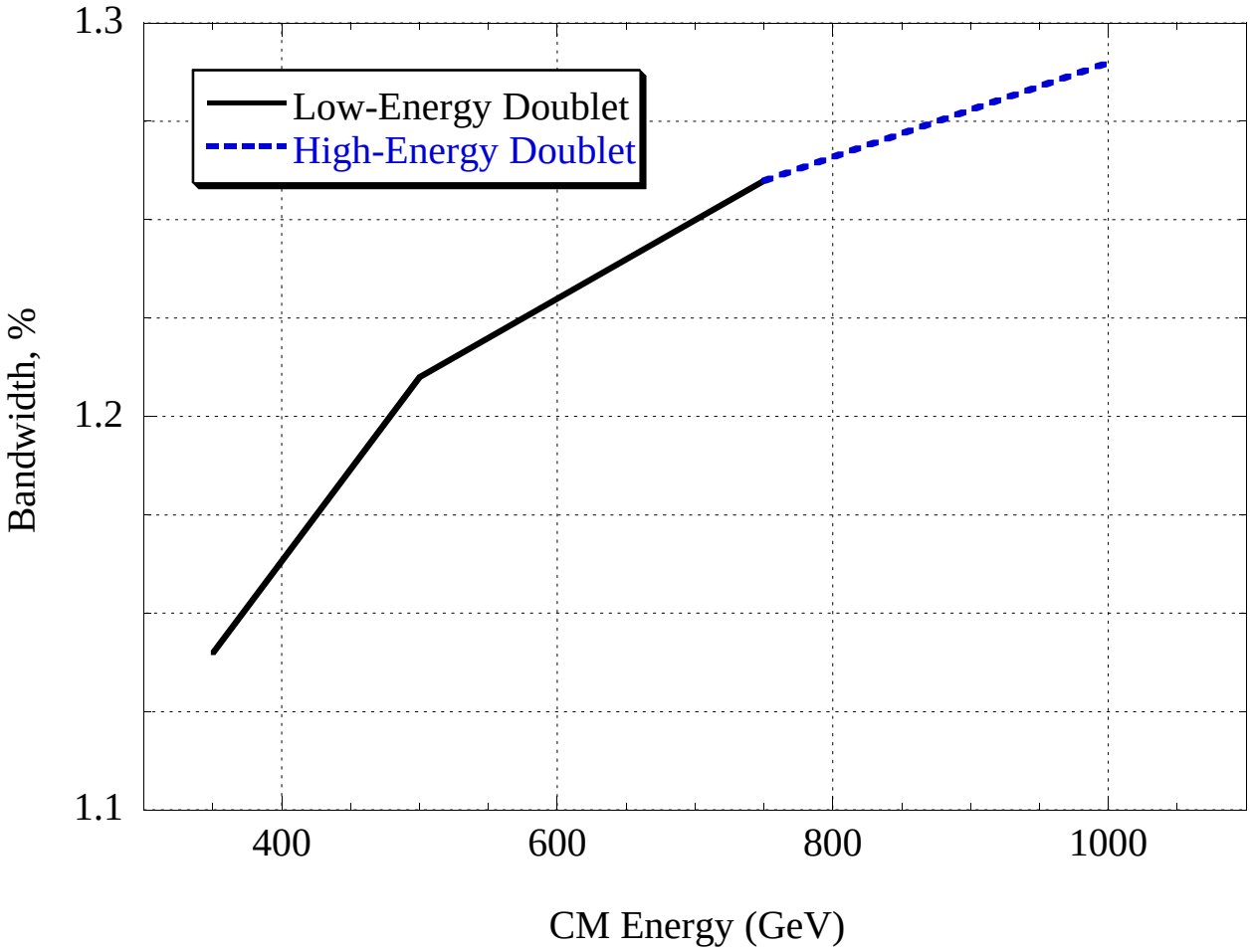

Figure 18: Bandwidth as a function of center-of-mass energy.

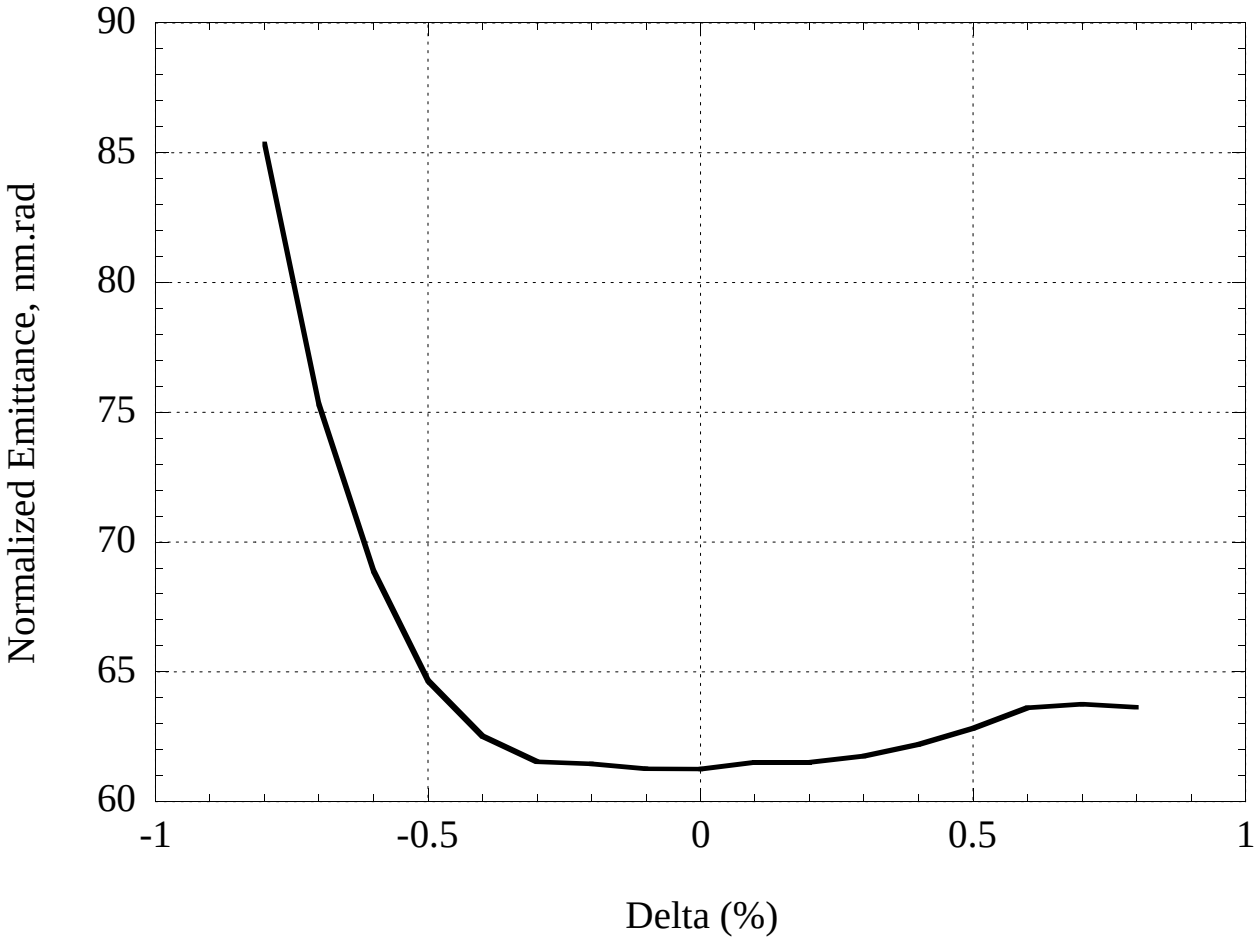

Figure 19: Vertical emittance at the IP for a monochromatic beam as a function of centroid energy offset.

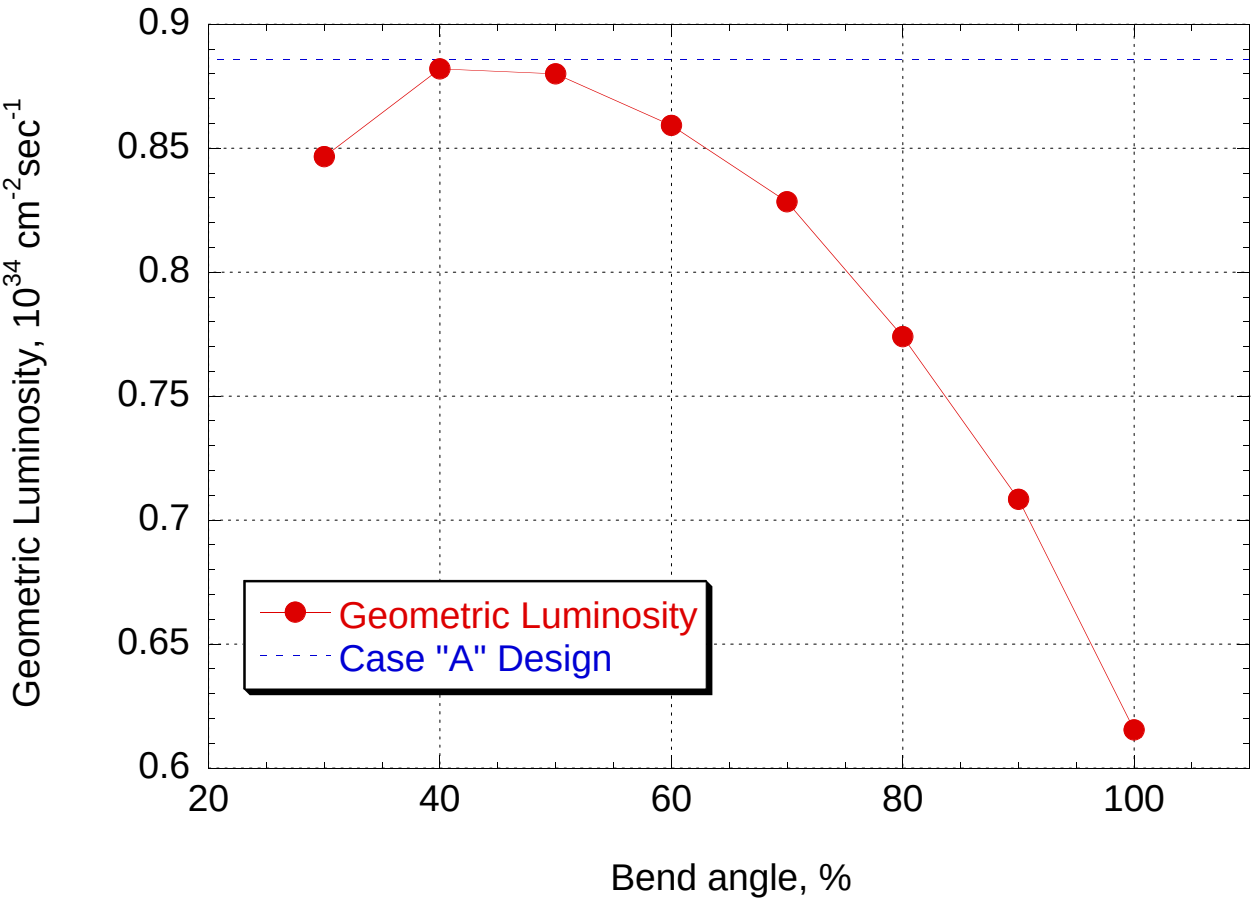

Figure 20: Luminosity as a function of final focus bend angle for 1.5 TeV CM.

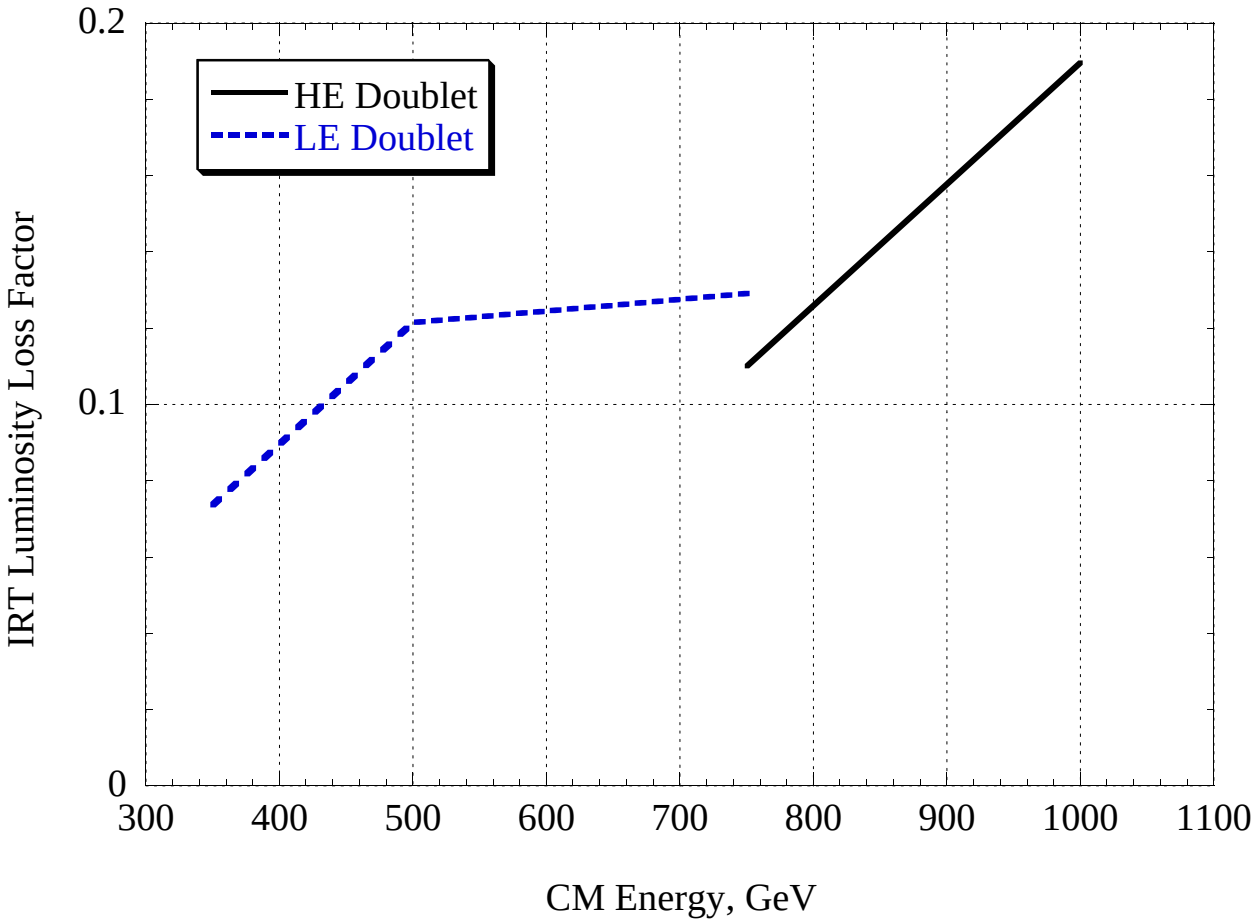

Figure 21: Fraction of expected luminosity lost as a function of CM energy. The "expected" luminosity was computed from the linear monochromatic IP spot sizes.

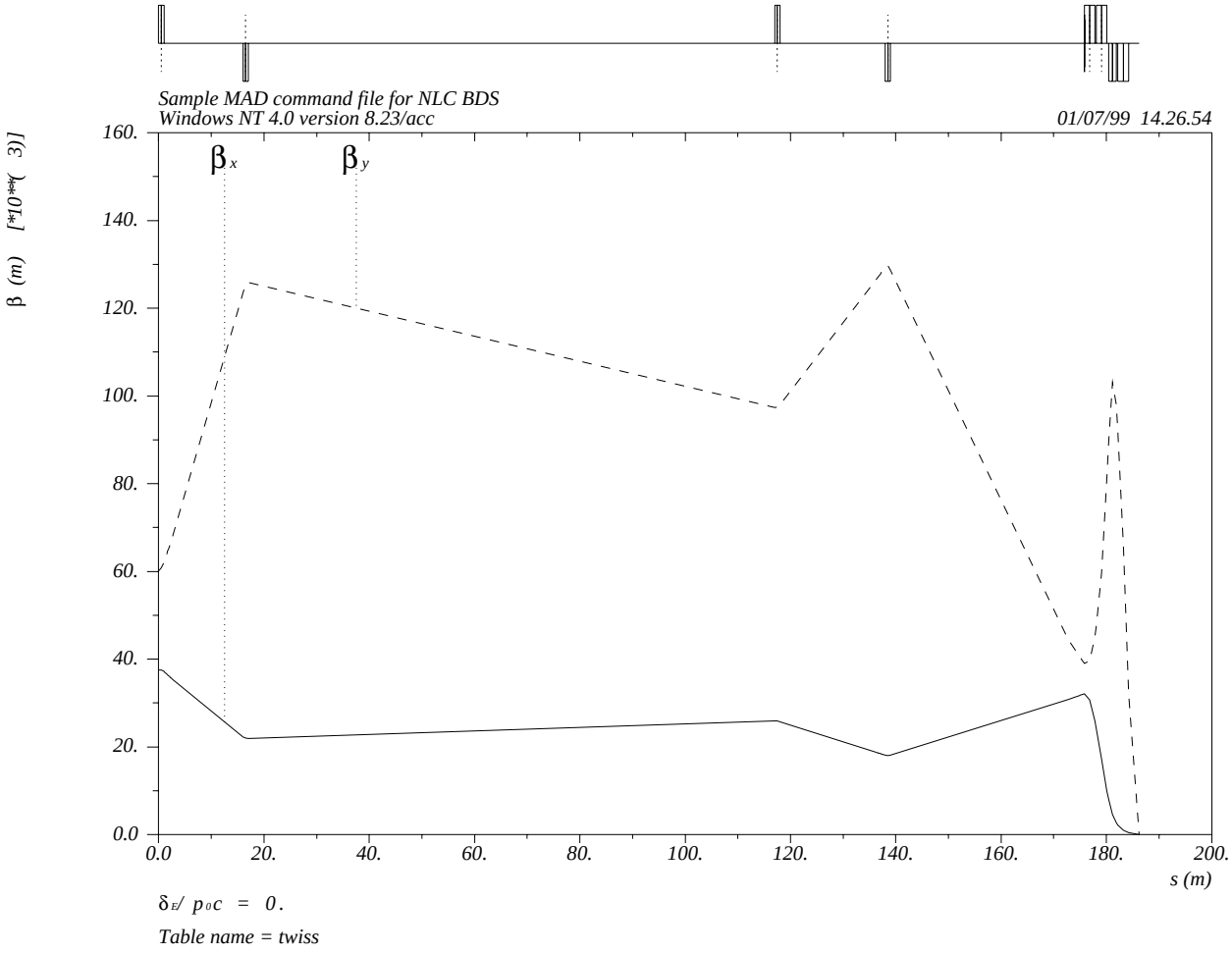

Figure 22: Final transformer Twiss functions.

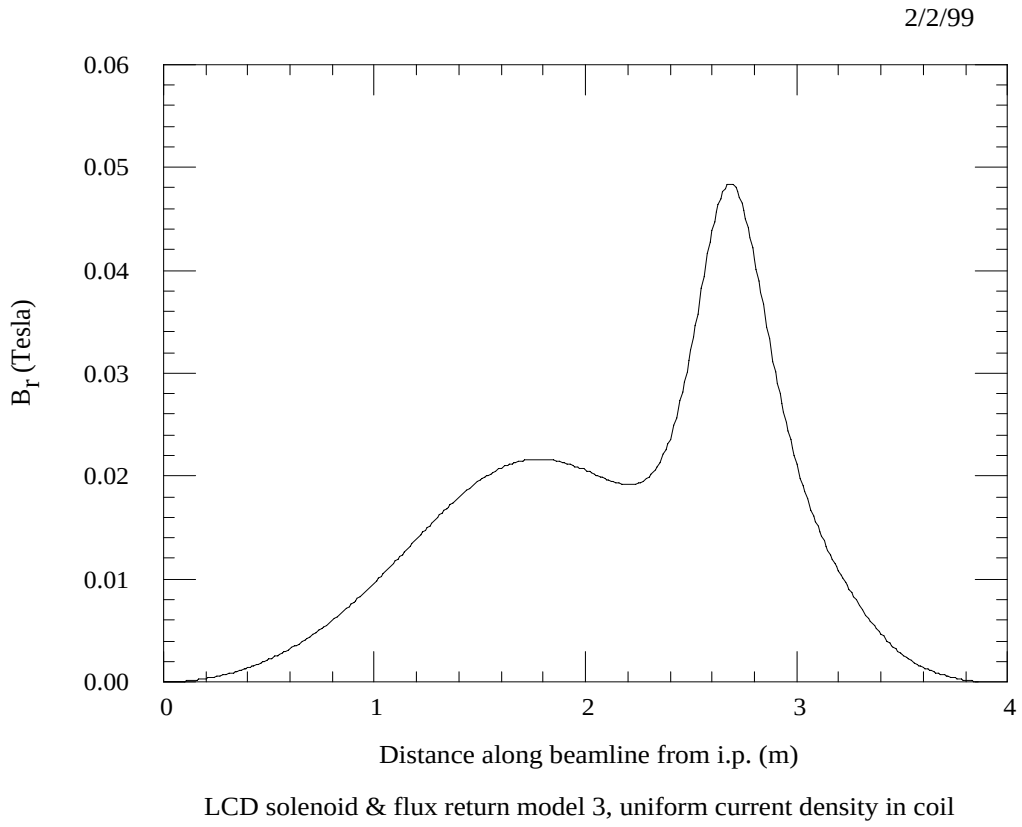

Figure 23: Radial magnetic field along the beam trajectory due to 6 T detector solenoid.

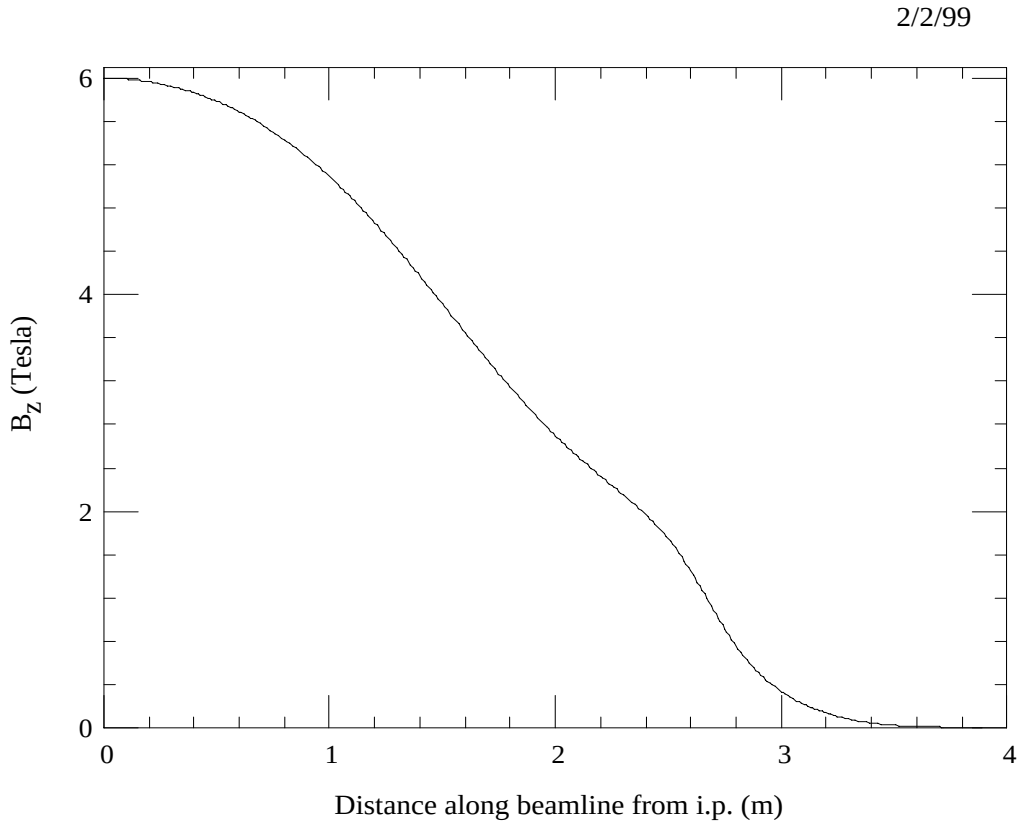

Figure 24: Longitudinal magnetic field along the beam trajectory due to 6 T detector solenoid.